



# International Journal for Innovative Engineering and Management Research

A Peer Reviewed Open Access International Journal

www.ijiemr.org

## COPY RIGHT

**2018 IJIEMR.** Personal use of this material is permitted. Permission from IJIEMR must be obtained for all other uses, in any current or future media, including reprinting/republishing this material for advertising or promotional purposes, creating new collective works, for resale or redistribution to servers or lists, or reuse of any copyrighted component of this work in other works. No Reprint should be done to this paper, all copy right is authenticated to Paper Authors

IJIEMR Transactions, online available on 13<sup>th</sup> Mar 2018. Link

[:http://www.ijiemr.org/downloads.php?vol=Volume-7&issue=ISSUE-03](http://www.ijiemr.org/downloads.php?vol=Volume-7&issue=ISSUE-03)

Title: **A FUZZY BASED TRANSFORMER LESS ACTIVE POWER FILTER WITH UPS FEATURES**

Volume 07, Issue 03, Pages: 40–53.

Paper Authors

**T. YAMUNA, Mr.S.DAMODHARAO**

Gonna Institute of Information Technology & Sciences, Visakhapatnam (Dt); Andhra Pradesh, India



USE THIS BARCODE TO ACCESS YOUR ONLINE PAPER

To Secure Your Paper As Per **UGC Guidelines** We Are Providing A Electronic Bar Code

## A FUZZY BASED TRANSFORMER LESS ACTIVE POWER FILTER WITH UPS FEATURES

<sup>1</sup>T. YAMUNA, <sup>2</sup>Mr.S.DAMODHARAO

<sup>1</sup>M-tech student ,Department of Electrical & Electronics Engineering, Gonna Institute of Information Technology & Sciences,Visakhapatnam (Dt); Andhra Pradesh, India.

<sup>2</sup>Assistant Professor, Department of Electrical & Electronics Engineering,Gonna Institute of Information Technology & Sciences,Visakhapatnam (Dt); Andhra Pradesh, India.

**Abstract:** In the modern power distribution system, majority of loads draw reactive power and/or harmonic currents from ac source along with main active power currents. These non-unity power factor linear and non-linear loads cause low efficiency of supply system, poor power-factor, destruction of other equipments due to excessive stresses and EMI problems. Active filters are widely employed in distribution system to reduce the harmonics produced by non-linear loads result in voltage distortion and leads to various power quality problems. In this work the simulation study of a fuzzy logic controlled based shunt active power filter capable of reducing the total harmonic distortion is presented. The advantage of fuzzy control is that it is based on a linguistic description and does not require a mathematical model of the system and it can adapt its gain according to the changes in load. Uninterrupted power supplies are widely used to supply critical loads and provide reliable and high quality energy to the load. Static UPS systems are the most commonly used UPS systems. They have a broad variety of applications from low-power personal computer and telecommunication systems, to medium-power medical systems, and to high-power utility systems. The main advantages are high efficiency, high reliability, and low total harmonic distortion (THD). The static UPS systems are classified into online, offline, and line-interactive. In extension we are replacing PI controller with fuzzy to reduce source current THD

### I INTRODUCTION

The requirements of quality at power grids and increased sensitivity of the loads has stimulated the use of power electronics in context of power line conditioning [1]. Different equipments are used to improve the power quality, e.g., transient suppressors, line voltage regulators, uninterrupted power supplies, active filters, and hybrid filters. The continuous proliferation of electronic equipments either

for home appliance or industrial use has the drawback of increasing the non sinusoidal current into power grid. So, the need for economical power conditioners for single-phase systems is growing rapidly [2]. Different solutions are currently proposed and used in practice applications to work out the problems of harmonics in electric grids. In the last decades, the use of active filtering techniques has become more attractive due

to the technological progress in power electronic switching devices and more efficient control algorithms. The issue of reducing the cost has been attracting the attentions of researchers. Generally, the largest cost reduction is achieved by reducing the number of switches employed in a power converter or developing topologies that employ switches with lower voltage stresses. Cost reduction is also achieved by eliminating passive components such as inductors, capacitors, and transformers. Reducing the numbers of switches and passive elements in active power filters (APF) and uninterruptible power supplies (UPS) topologies not only reduces the cost of the whole system but also provides some other advantages such as great compactness, smaller weight, and higher reliability. However, the cost reduction requires the use of more complex control strategies. Uninterrupted power supplies are widely used to supply critical loads and provide reliable and high quality energy to the load. Static UPS systems are the most commonly used UPS systems. They have a broad variety of applications from low-power personal computer and telecommunication systems, to medium-power medical systems, and to high-power utility systems. The main advantages are high efficiency, high reliability, and low total harmonic distortion (THD). The static UPS systems are classified into online, offline, and line-interactive. This study will focus on the study of series-parallel line interactive UPS topology, also known as delta converter, with reduced number of switches. The idea consists in developing a

reconfigurable structure where one of the converter leg can be used to charge the battery bank without having a dedicated dc/dc converter, e.g., buck-boost converter. So, the configuration composed by the four-leg converter can operate with three leg leaving one leg to charge the battery bank. When the battery bank is charged, the system returns to its original form. A mathematical modeling and complete control system, including the pulse width modulation (PWM) techniques, is presented. Simulated and experimental results validate the theoretical considerations.

## II SYSTEMS MODELING

The proposed configuration shown in Fig.1 (a) comprise the grid ( $e_g, i_g$ ), internal grid inductance ( $L_g$ ), load  $Z_l$  ( $v_l, i_l$ ), converters  $S_e$  and  $S_h$  with a capacitor bank at the dc-link and filters  $Z_e$  ( $L_e, L'_e, \text{ and } C_e$ ) and  $Z_h$  ( $L_h, L'_h, \text{ and } C_h$ ). Converter  $S_e$  is composed by switches  $q_e, \bar{q}_e, q'_e, \text{ and } \bar{q}'_e$ . Converter  $S_h$  is composed by switches  $q_h, \bar{q}_h, q'_h, \text{ and } \bar{q}'_h$ . The conduction state of all switches is represented by an homonymous binary variable, where  $q=1$  indicates a closed switch, while  $q=0$  an open one.

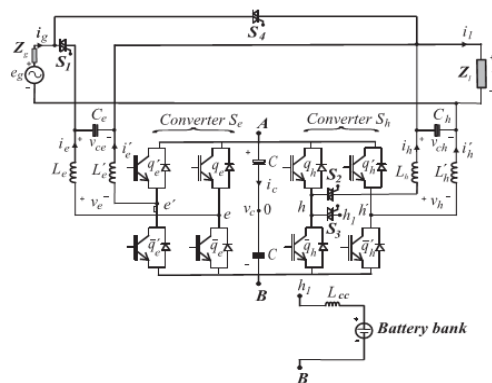


Fig.1 (a) Single-phase universal active filter proposed topology with UPS features.

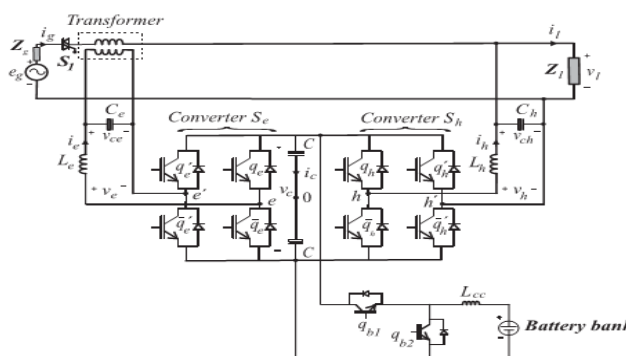


Fig.1 (b) Single-phase universal active filter conventional topology with UPS features.

The difference between the two systems, Fig.1, relates to components reduction. The proposed configuration, Fig.1 (a), is transformerless and presents less power switches than the conventional, Fig.1 (b). The idea of the proposed system is to utilize one of the converter leg to charge the battery bank when dc voltage level at the battery bank is beyond the preset tolerance avoiding the necessity to have a dedicated dc/dc buck-boost converter for it. The buck-boost converter of the conventional topology is composed by switches  $q_{b1}$  and  $q_{b2}$ . The filter inductance  $L_{cc}$  is common to both configurations. The system description with the power converter operating with four and three leg is addressed.

### 1 Four-Leg Converter Operation Mode

The converter pole voltages  $v_{e0}$ ,  $v'_{e0}$ ,  $v_{h0}$ , and  $v'_{h0}$  depend on the conduction states of the power switches, that is

$$v_{e0} = (2q_e - 1) \frac{v_c}{2} \quad (1)$$

$$v'_{e0} = (2q'_e - 1) \frac{v_c}{2} \quad (2)$$

$$v_{h0} = (2q_h - 1) \frac{v_c}{2} \quad (3)$$

$$v'_{h0} = (2q'_h - 1) \frac{v_c}{2} \quad (4)$$

Where  $v_c$  is the dc-link voltage.

From Fig.1 (a), assuming that the switches  $S_1$  and  $S_2$  are ON and  $S_3$  and  $S_4$  are OFF, the following equations can be derived considering the system operating with four leg.

$$v_{e0} - v'_{e0} = v_g + \left[ \frac{r'_e}{2} + \frac{r_e}{2} + \left( \frac{l_e}{2} + \frac{l'_e}{2} \right) p \right] i_e - v_l - \left( \frac{r'_e}{2} + \frac{l'_e}{2} p \right) i_o \quad (5)$$

$$pv_{ce} = \frac{1}{C_e} (i_g + i_e) \quad (6)$$

$$pv_l = \frac{1}{C_h} (i_g - i_l + i_h + i_o) \quad (7)$$

Where  $p=d/dt$ ,  $v_g = e_g - r_g i_g - l_g p i_g$ ,  $v_l = v_{ch}$  and  $i_l$  is calculated using the load model, which can be linear or nonlinear; and symbols like  $r$  and  $l$  represent resistances and inductances of the inductors  $L_g$ ,  $L_e$ ,  $L'_e$ ,  $L_h$ , and  $L'_h$ . The circulating current  $i_o$  is defined by

$$i_o = i_e + i'_e = -(i_h + i'_h). \quad (8)$$

The resultant circulating voltage model is obtained by adding (5)–(8)

The voltage  $v_o$  is used to compensate the circulating current  $i_o$ . The demonstration of this current can be seen in. From the point of view of the controllers, the voltages:  $v_e = v_{e0} - v'_{e0}$  (converter  $S_e$ ) is used to regulate and compensate the load voltage  $v_l$ ,  $v_h = v_{h0} - v'_{h0}$  (converter  $S_h$ ) regulates and controls the grid current in order to maintain the power factor close to one and  $v_o = v'_{e0} + v_{e0} - v'_{h0} - v_{h0}$  (converter  $S_e + S_h$ ) is used to cancel or gather the circulating current  $i_o$  near to zero.

In the balanced case, filter inductors are equal ( $L_e = L'_e$  and  $L_h = L'_h$ ) and the circulating voltage model become more simple, that is

$$v_o = v_g + \left[ \left( \frac{r_e}{2} + \frac{r_h}{2} \right) + \left( \frac{l_e}{2} + \frac{l_h}{2} \right) p \right] i_o \quad (9)$$

Thus, it can be noted that to minimize the circulating current  $i_o$ , the voltage  $v_o$  must be equal to  $v_g$ , i.e.

$$v_o = v_g \quad (10)$$

## 2 Three-Leg Converter Operation Mode

The system composed by three leg works similar but, in this case, it has a shared leg used by both converters (series and parallel filter) and a free leg, which is used to charge the battery bank when needed. The converter pole voltages  $v'_{e0}$ ,  $v_{h0}$ , and  $v'_{h0}$  depend on the conduction states of the power switches and may be expressed as

$$v'_{e0} = (2q'_e - 1) \frac{v_c}{2} \quad (11)$$

$$v_{e0} = (2q_e - 1) \frac{v_c}{2} \quad (12)$$

$$v'_{h0} = (2q'_h - 1) \frac{v_c}{2} \quad (13)$$

Assuming that the system operates with three legs and considering that the switches  $S_1$  and  $S_3$  are ON and  $S_2$  and  $S_4$  are OFF, following equations can be obtained:

$$v_{e0} - v'_{e0} = v_g - v_l + \left( \frac{r_e}{2} + \frac{l_e}{2} p \right) i_e - \left( \frac{r'_e}{2} + \frac{l'_e}{2} p \right) i'_e \quad (14)$$

$$pv_{ce} = \frac{1}{C_e} (i_g + i_e) \quad (15)$$

$$pv_l = \frac{1}{C_h} (i_g - i_l) \quad (16)$$

Where  $p = d/dt$ ,  $v_g = e_g - r_g i_g - l_g p i_g$ ,  $v_l = v_{ch}$ , and  $i_l$  is calculated using the load model, which can be linear or nonlinear. For this case, it is noted by the equations that there is no circulation current  $i_o$ .

## III PWM STRATEGY

This section presents the PWM Strategy for different modes of operations. First, the system starts as four-leg converter and when is need to charge the bank of batteries it is reconfigurable to operate as three leg. The descriptions of these modes of operations are presented as following.

## 1 Four-Leg Converter Operation Mode

Pulse widths of gating signals can be directly calculated from the pole voltages  $v_{e0}^*$ ,  $v_{e0}^*$ ,  $v_{h0}^*$ , and  $v_{h0}^*$ . Considering that  $v_e^*$ ,  $v_h^*$ , and  $v_0^*$  denote the reference voltages requested by the controllers, it comes

$$v_{e0}^* - v_{e0}^* = v_e^* \quad (17)$$

$$v_{h0}^* - v_{h0}^* = v_h^* \quad (18)$$

$$v_{e0}^* + v_{e0}^* - v_{h0}^* - v_{h0}^* = v_0^* \quad (19)$$

Such equations are sufficient to determine the four pole voltages  $v_{e0}^*$ ,  $v_{e0}^*$ ,  $v_{h0}^*$ , and  $v_{h0}^*$ . Introducing an auxiliary variable  $v_x^*$  and choosing  $v_{e0}^* = v_x^*$ , it can be written

$$v_{e0}^* = v_e^* + v_x^* \quad (20)$$

$$v_{e0}^* = v_x^* \quad (21)$$

Two methods are presented in order to choose  $v_x^*$ .

### 1) Method A: General Approach

In this approach, the reference voltage  $v_x^*$  is calculated by taking into account the maximum  $v_c^*/2$  and minimum

$-v_c^*/2$  value of the pole voltages, then

$$v_{x \max}^* = v_c^*/2 - v_{\max}^* \quad (22)$$

$$v_{x \min}^* = -v_c^*/2 - v_{\min}^* \quad (23)$$

Where  $v_c^*$  is the reference dc-link voltages,  $v_{\max}^* = \max \vartheta$  and  $v_{\min}^* = \min \vartheta$  with  $\vartheta = \{v_e^*, 0, v_e^*/2 + v_h^*/2 - v_0^*/2, v_e^*/2 - v_h^*/2 - v_0^*/2\}$

After  $v_x^*$  is selected, all pole voltages are obtained from,  $v_x^*$  can be chosen equal to  $v_{x \max}^*$ ,  $v_{x \min}^*$ , or  $v_{x \text{ave}}^* = (v_{x \max}^* + v_{x \min}^*)/2$ . Note that when  $v_{x \max}^*$  or  $v_{x \min}^*$  is selected, one of the converter leg operates with zero switching frequency. On the other hand, operation with  $v_{x \text{ave}}^*$  generates pulse voltage centered in the sampling period that can improve the THD of voltages.

### 2) Method B: Local Approach

In this case, the voltage  $v_{xs}^*$  is calculated by taking into account its maximum and minimum values in the series or shunt side. For example, if the series side is considered ( $s = e$ ), then  $v_{xe \max}^* = \max \vartheta_e$  and  $v_{xe \min}^* = \min \vartheta_e$  with  $\vartheta_e = \{v_e^*, 0\}$  and if the shunt side ( $x = h$ ) is considered  $v_{xh \max}^* = \max \vartheta_h$  and  $v_{xh \min}^* = \min \vartheta_h$  with  $\vartheta_h = \{v_e^*/2 + v_h^*/2 - v_0^*/2, v_e^*/2 - v_h^*/2 - v_0^*/2\}$ . Besides these voltages, voltage  $v_x^*$  must also obey the other converter side. Then, these limits can be obtained directly from  $v_{x \max}^*$  and  $v_{x \min}^*$

The algorithm for this case is given by

- 1) Choose the converter side to be the THD optimized and calculate  $v_{xs}^*$  between  $v_{xs \max}^*$ ,  $v_{xs \min}^*$  or  $v_{xs \text{ave}}^* = (v_{xs \max}^* + v_{xs \min}^*)/2$ ;
- 2) calculate the limits  $v_{x \max}^*$  and  $v_{x \min}^*$

- 3) do  $v_{xs}^* = v_{xmax}^*$  if  $v_{xs}^* > v_{xmax}^*$  and  $v_{xs}^* = v_{xmin}^*$  if  $v_{xs}^* < v_{xmin}^*$ ;
- 4) do  $v_x^* = v_{xs}^*$ ;
- 5) Determine the pole voltage and the gating signal as in previous method.

## 2 Three-Leg Converter Operation Mode

The pulse widths of the gating signals can be directly calculated from the voltage referred to the dc-bus midpoint, which is given by the desired voltages for the grid and loads. If the desired phase voltages are specified as  $v_e^*$  e  $v_h^*$ , then the reference midpoint voltages can be expressed as

$$v_{e0}'^* = v_e^* + v_{e0}^* \quad (24)$$

$$v_{h0}'^* = v_h^* + v_{e0}^*. \quad (25)$$

### 1) Method A: General Approach

The voltage  $v_\mu^*$  can be calculated taking into account the general apportioning factor  $\mu$  that is

$$v_\mu^* = E \left( \mu - \frac{1}{2} \right) - \mu v_{max}^* + (\mu - 1) v_i^* \quad (26)$$

Where  $v_{max}^* = \max(v_e^*, v_h^*, 0)$  and  $v_{min}^* = \min(v_e^*, v_h^*, 0)$ .

The apportioning factor  $\mu$  ( $0 \leq \mu \leq 1$ ) is given by

$$\mu = \frac{t_{oi}}{t_o} \quad (27)$$

and indicates the distribution of the general free-wheeling period  $t_o$  (period in which voltages  $v_{e0}'^*$ ,  $v_{h0}'^*$ , and  $v_{e0}^*$  are equals) between the beginning ( $t_{oi} = \mu t_o$ ) and the end ( $t_{of} = (1-\mu) t_o$ ) of the switching period.

The apportioning factor can be changed as a function of the modulation index ( $\mu$ ) to reduce the THD of both converter voltages.

In this case, the proposed algorithm is

- 1) Choose the general apportioning factor  $\mu$  and calculate  $v_\mu^*$  from (3.48);
- 2) Determine  $v_{e0}'^*$ ,  $v_{h0}'^*$ , and  $v_{e0}^*$  from (3.45)–(3.47);
- 3) Finally, once the midpoint voltage have been determined, calculate pulse widths  $\tau_e$ ,  $\tau_e'$ , and  $\tau_h'$

### 2) Method B: Local Approach

The voltage  $v_\mu^*$  can be calculated taking into account the local apportioning factor  $\mu_s$ :

- 1) For the grid  $\mu_s = \mu_e$ , dividing (splitting) the period  $t_{oe}$ , in which the voltages  $v_{e0}'^*$  and  $v_{e0}^*$  are equal, at the beginning ( $t_{oie} = \mu_e t_{oe}$ ) and at the end ( $t_{ofe} = (1-\mu_e) t_{oe}$ ) of the switching period;
- 2) For the load  $\mu_s = \mu_h$ , splitting the period  $t_{oh}$ , in which the voltages  $v_{h0}'^*$  and  $v_{e0}^*$  are equal, at the beginning ( $t_{oih} = \mu_h t_{oh}$ ) and at the end ( $t_{ofh} = (1-\mu_h) t_{oh}$ ) of the switching period.

Thus, the reference voltage  $v_\mu^*$  can be expressed by

$$v_{\mu s}^* = E \left( \mu_s - \frac{1}{2} \right) - \mu_s v_{smax}^* + (\mu_s - 1) v_{smin}^* \quad (28)$$

Where  $v_{smax}^* = \max V_e$  and  $v_{smin}^* = \min V_g$  if  $s = e$  or  $v_{smax}^* = \max V_h$  and  $v_{smin}^* = \min V_h$  if  $s = h$ , where  $V_e = \{v_e^*, 0\}$  and  $V_h = \{v_h^*, 0\}$ . Besides (3.53), the voltage  $v_{\mu s}^*$  must also obey the other converter side.

In this case, it is possible to control how the harmonic distortion is divided by

both converters. So, the proposed algorithm is

- 1) Choose the local apportioning factor  $\mu_s$  so that grid or load converter is optimized; calculate  $v_{\mu s}^*$  from (3.48);
- 2) Determine  $v_{e0}^*$ ,  $v_{h0}^*$ , and  $v_{e0}^*$  from (45)–(47) using  $v_{\mu}^* = v_{\mu s}^*$ ;
- 3) Use Step 3 of Method A.

## IV OVERALL CONTROL STRATEGY

As mentioned in the previous sections, the modes of operation of the converter are defined by the system functionality. The system can operate with four or three leg depend on the need; or in case of grid voltage fault, the battery bank is used to supply energy to the dc-bus capacitor voltage and inverter in order to maintain the desirable voltage to the load. The description of the operation mode of the proposed circuit can be observed at Fig.3.2. The image in gray represents the section of the circuit that is not in use. Four operation modes are presented. In Fig.3.2 (a), the system operates with four leg. In three-leg mode, presented at Fig.3.2 (b), the free leg denoted by his not in use. At Fig.3.2 (c), the system is still operating in three-leg mode and the free leg is used to charge the battery bank, operating as buck converter. Finally, assuming the battery charged, Fig.3.2 (d) presents the condition in which the energy is transferred from the battery bank to the load via an inverter, considering the failure at the ac input. At this mode, the leg  $h$  works as boost converter.

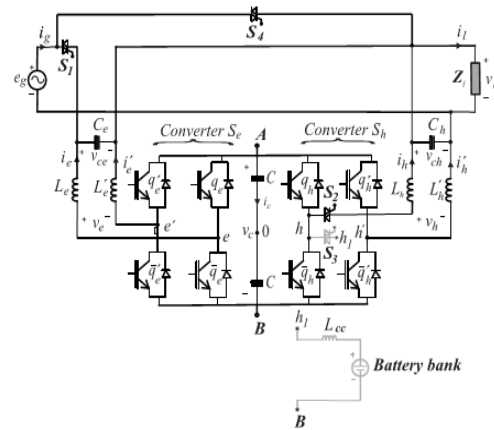


Fig..2 (a) four-leg mode

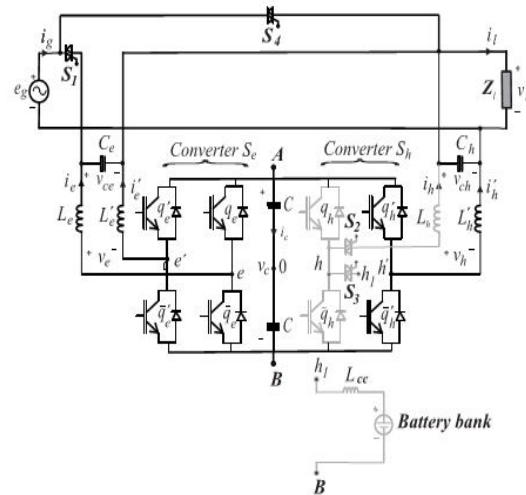


Fig..2 (b) three-leg mode

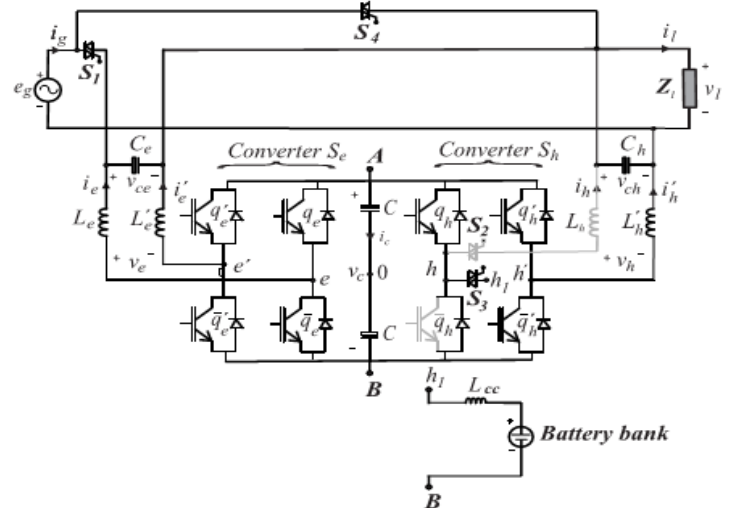


Fig..2 (c) three-leg mode charging the battery bank

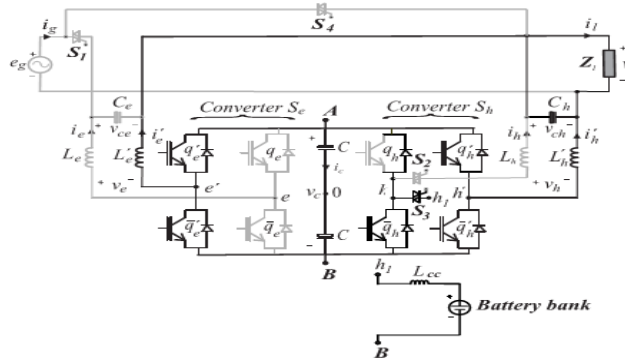


Fig.2 (d) failure at the ac input  
 Fig.2 Description of modes of operations

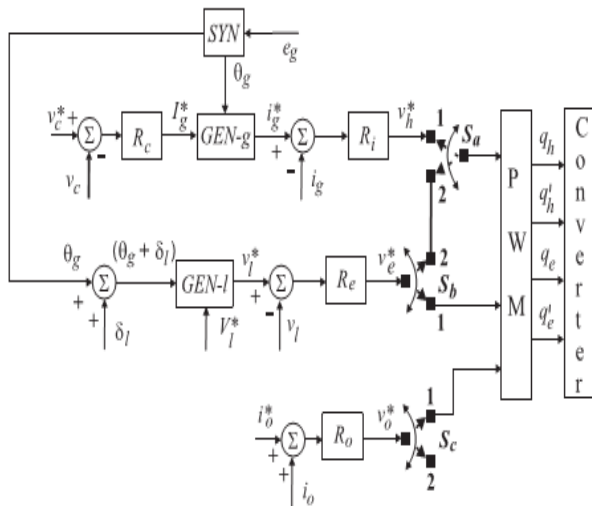


Fig.3. Control block diagram of the proposed configuration.

The proposed system control is shown in fig 3. The mode of operation of the converter is determined by the state of switch  $S_c$ . If  $S_c$  is in position 1, the converter operates according to the four-leg mode. If  $S_c$  is in position 2, the selected mode is three leg. The disconnection of the circulating current control block makes possible to use the shared leg to charge the battery bank. For the system operating with four leg, switches  $S_a$ ,  $S_b$ , and  $S_c$  in position 1, the capacitor dc-link voltage  $v_c$  ( $v_c = E$ ) is adjusted to a reference value by using the controller  $R_c$ , which is a standard PI type controller. This

controller provides the amplitude of the reference current  $I_g^*$ . For the power factor and harmonic control, the instantaneous reference current  $i_g^*$  must be synchronized with voltage  $e_g$ . This is performed by the block GEN-g, from a PLL scheme. From the synchronization with  $e_g$  and the amplitude  $I_g^*$ , the current  $i_g^*$  is generated. The current controller is implemented by using the controller indicated by block  $R_i$ . The controller  $R_i$  is a double sequence digital current controller employed in [21]. Thus, current controller defines the input reference voltage  $v_h^*$ . The instantaneous reference load voltage  $v_l^*$  can be determined by using the rated optimized load angle  $\delta_l$  plus the information  $\theta_g$  from block SYN and the defined load amplitude  $v_l^*$ . The block GEN-l uses the input information to generate the desired reference load voltage  $v_l^*$ . The homo-polar current  $i_o$  is controlled by controller  $R_o$ , that determines voltage  $v_o^*$  responsible to minimize the effect of the circulating current  $i_o$ , maintaining this current near to zero. All these voltages are applied to PWM block to determine the conduction states of the converter's switches. When the switch  $S_c$  is in position 2, three-leg mode of operation occurs. The dc/dc buck converter is used to charge the battery bank. The free leg makes the dc-bus voltage  $V_{cc}$  to be stepped down in its average value to supply the dc-battery bank according to  $V_{bat} = DV_{cc}$ . The battery voltage  $V_{bat}$  is directly proportional to duty ratio  $D$ . In the stored-energy mode of operation, when the ac input voltage is beyond the permissible tolerance range, the switch  $S_l$  disconnects the ac input,

transferring the energy from the battery bank to the load via an inverter. Since the battery voltage is low, it is first required to be boosted to high dc voltage for the proper operation of the dc/ac inverter, now responsible to supply the load. The low battery voltage  $V_{bat}$  is boosted to high dc voltage  $V_{cc}$  according to  $V_{cc} = V_{bat} / (1-D)$ . When both switches  $S_a$  and  $S_b$  are in position 2, situation in which the ac input voltage fail, the load is supplied by the battery bank and inverter. At this point, the converter  $S_h$  that was responsible for regulating the grid current and the dc-bus voltage is now responsible for maintaining the voltage applied to the load.

#### IV INTRODUCTION TO FUZZY LOGIC CONTROLLER

L. A. Zadeh presented the first paper on fuzzy set theory in 1965. Since then, a new language was developed to describe the fuzzy properties of reality, which are very difficult and sometime even impossible to be described using conventional methods. Fuzzy set theory has been widely used in the control area with some application to dc-to-dc converter system. A simple fuzzy logic control is built up by a group of rules based on the human knowledge of system behavior. Matlab/Simulink simulation model is built to study the dynamic behavior of dc-to-dc converter and performance of proposed controllers. Furthermore, design of fuzzy logic controller can provide desirable both small signal and large signal dynamic performance at same time, which is not possible with linear control technique. Thus, fuzzy logic controller has been potential ability to improve the robustness of dc-to-dc

converters. The basic scheme of a fuzzy logic controller is shown in Fig 5 and consists of four principal components such as: a fuzzification interface, which converts input data into suitable linguistic values; a knowledge base, which consists of a data base with the necessary linguistic definitions and the control rule set; a decision-making logic which, simulating a human decision process, infer the fuzzy control action from the knowledge of the control rules and linguistic variable definitions; a defuzzification interface which yields non fuzzy control action from an inferred fuzzy control action [10].

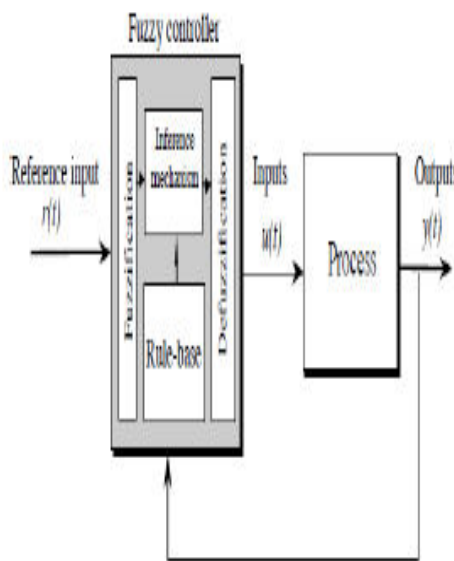


Fig.4. General Structure of the fuzzy logic controller on closed-loop system

The fuzzy control systems are based on expert knowledge that converts the human linguistic concepts into an automatic control strategy without any complicated mathematical model [10]. Simulation is performed in buck converter to verify the proposed fuzzy logic controllers.

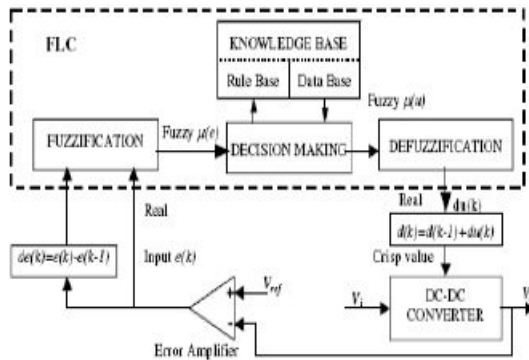


Fig.5. Block diagram of the Fuzzy Logic Controller (FLC) for dc-dc converters

### A. Fuzzy Logic Membership Functions:

The dc-dc converter is a nonlinear function of the duty cycle because of the small signal model and its control method was applied to the control of boost converters. Fuzzy controllers do not require an exact mathematical model. Instead, they are designed based on general knowledge of the plant. Fuzzy controllers are designed to adapt to varying operating points. Fuzzy Logic Controller is designed to control the output of boost dc-dc converter using Mamdani style fuzzy inference system. Two input variables, error (e) and change of error (de) are used in this fuzzy logic system. The single output variable (u) is duty cycle of PWM output.

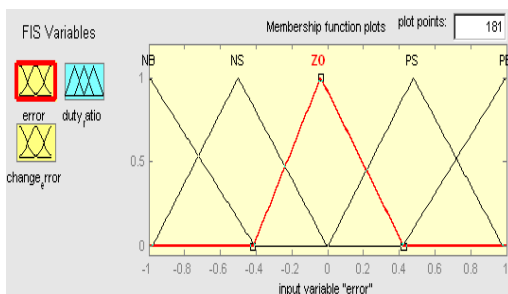


Fig. 6. The Membership Function plots of error

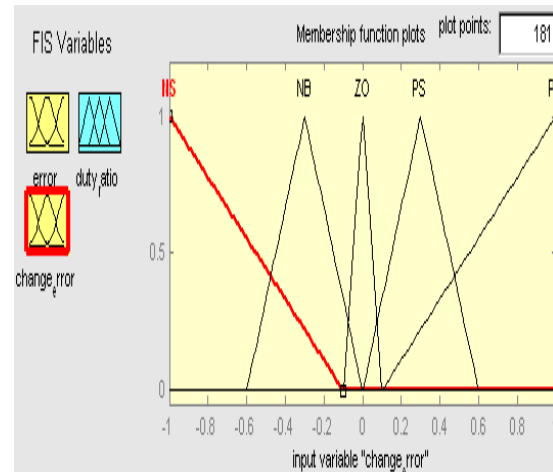


Fig.7. The Membership Function plots of change error

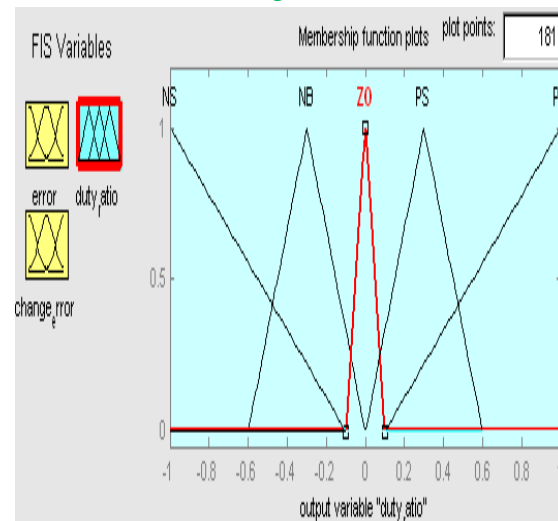


Fig.8. the Membership Function plots of duty ratio

### B. Fuzzy Logic Rules:

The objective of this dissertation is to control the output voltage of the boost converter. The error and change of error of the output voltage will be the inputs of fuzzy logic controller. These 2 inputs are divided into five groups; NB: Negative Big, NS: Negative Small, ZO: Zero Area, PS: Positive small and PB: Positive Big and its parameter [10]. These fuzzy control rules for error and

change of error can be referred in the table that is shown in Table I as per below:

Table I

Table rules for error and change of error

(de) \ (e)	NB	NS	ZO	PS	PB
NB	NB	NB	NB	NS	ZO
NS	NB	NB	NS	ZO	PS
ZO	NB	NS	ZO	PS	PB
PS	NS	ZO	PS	PB	PB
PB	ZO	PS	PB	PB	PB

## VI. MATLAB/SIMULATION RESULTS

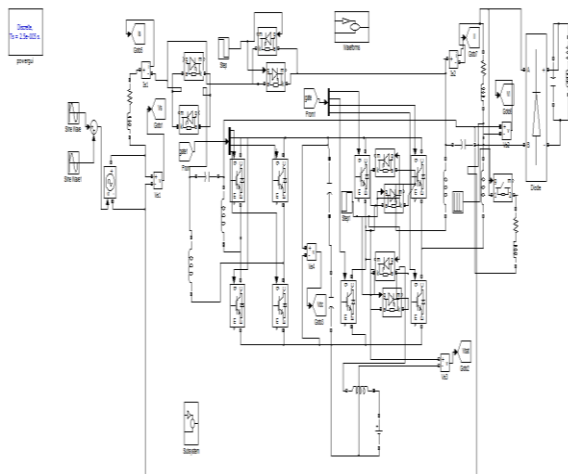


Fig 9 Matlab/simulation circuit of Single-phase universal active filter topologies with UPS features

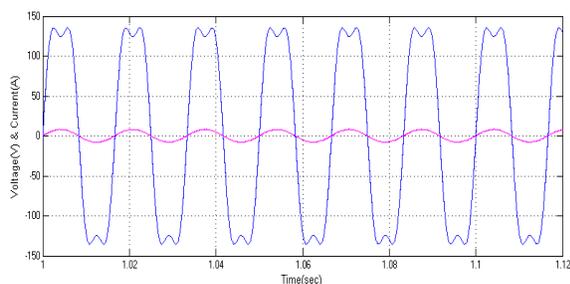


Fig 10 Simulation results of the proposed system: source voltage ( $e_g$ ) and source current ( $i_g$ )

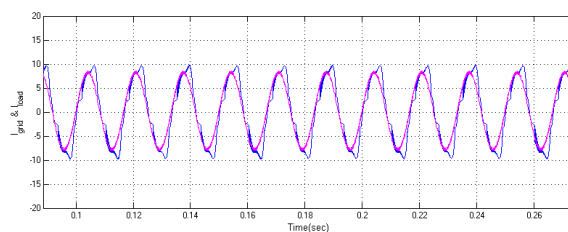


Fig 11 Simulation results of the proposed system: grid current ( $i_g$ ) and load current ( $i_l$ )

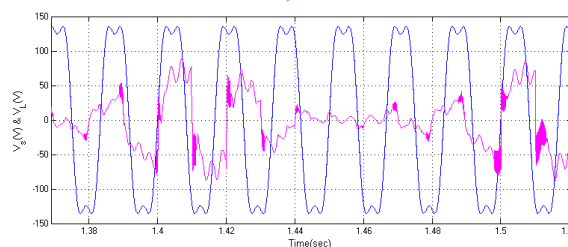


Fig 12 Simulation results of the proposed system: grid voltage ( $e_g$ ) and load voltage ( $v_l$ ).

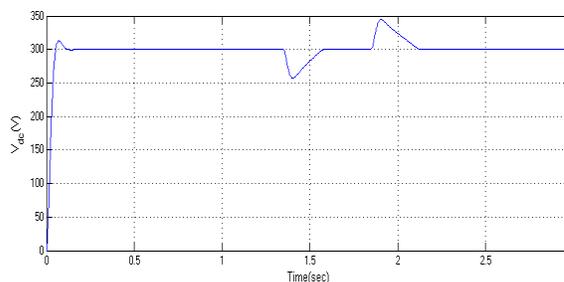


Fig 13 Simulation wave form of Single-phase universal active filter topologies with UPS

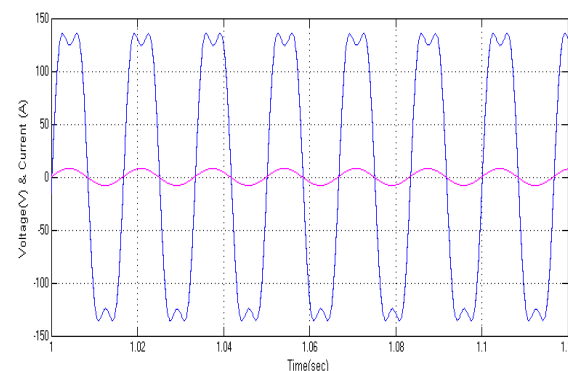


Fig 14 Simulation results of the proposed system: source voltage ( $e_g$ ) and source current ( $i_g$ ) with fuzzy logic controller

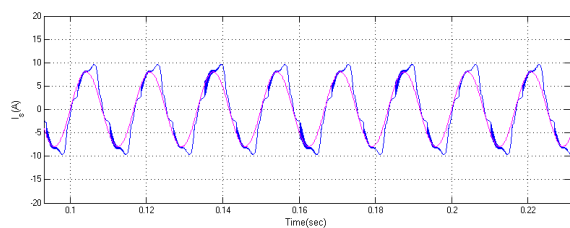


Fig 15 Simulation results of the proposed system: grid current ( $i_g$ ) and load current ( $i_l$ ) with fuzzy logic controller

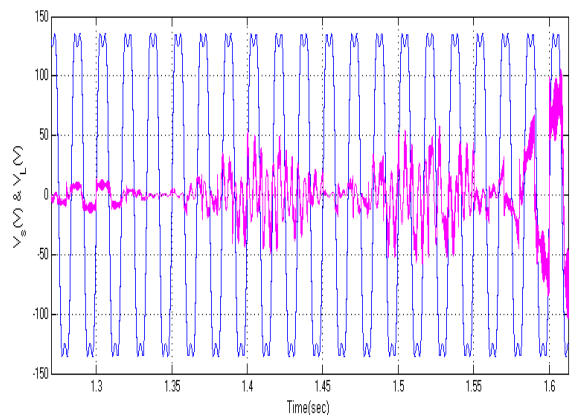


Fig 16 Simulation results of the proposed system: grid voltage ( $e_g$ ) and load voltage ( $v_l$ ) with fuzzy logic controller

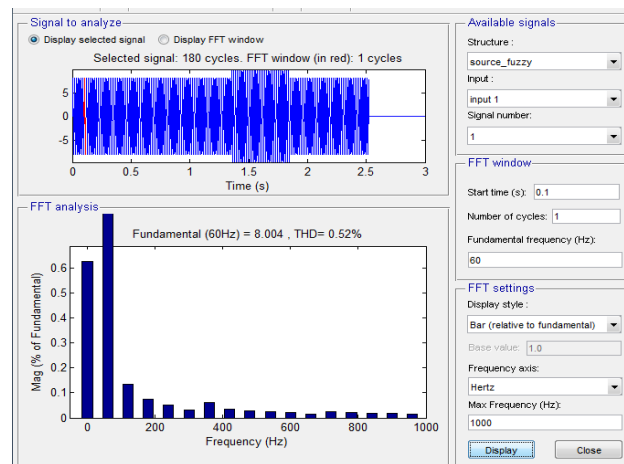


Fig 18 FFT analysis of THD with fuzzy logic controller

## CONCLUSION

An universal active power filter for harmonic and reactive power compensation with UPS features for a single-phase system has been presented. The proposed configuration is a transformerless delta converter with reduced number of components that emulates the buck–boost converter from the shared leg. The system modeling of the proposed system shows that the circulating current can be controlled to a level near to zero. The control of the circulating current is accomplished by the voltage (converters  $S_e + S_h$ ) in order to control the  $i_o$  close to zero. In the three-legs mode of operation, the circulating current does not exist. A suitable control strategy for the proposed system, including PWM techniques has also been presented. The system can be reconfigurable to operate with four or three leg leaving the free leg to charge the battery bank without having a dedicated dc/dc buck–boost converter. The configuration produces satisfactory results. The proposed solution has the advantage of reducing volume and cost in comparison to

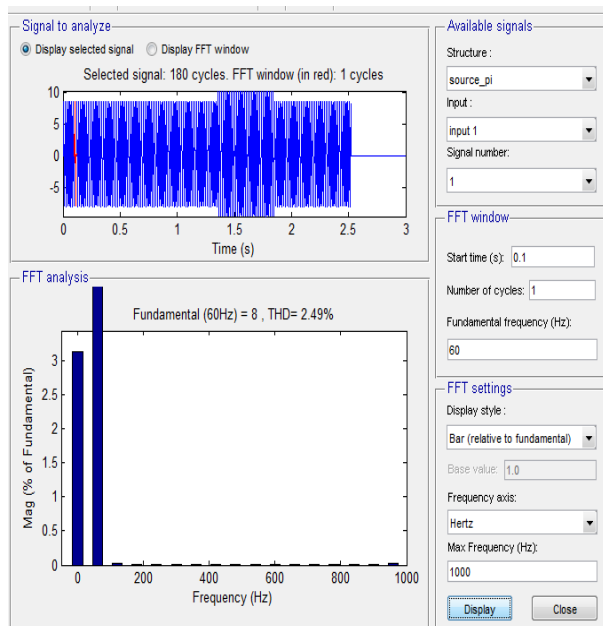


Fig 17 FFT analysis of THD with PI controller

the conventional UAPF. The proposed system with fuzzy logic controller the THD factor is reduced and system is more accurate.

## REFERENCES

- [1] H. Akagi, "Trends in active power line conditioners," *IEEE Trans. Power Electron.*, vol. 9, no. 3, pp. 263–268, May 1994.
- [2] B. Singh, K. Al-Haddad, and A. Chandra, "A review of active filters for power quality improvement," *IEEE Trans. Ind. Electron.*, vol. 46, no. 5, pp. 960–971, Oct. 1999.
- [3] Z. Pan, F. Z. Peng, and S. Wang, "Power factor correction using a series active filter," *IEEE Trans. Power Electron.*, vol. 20, no. 1, pp. 148–153, Jan. 2005.
- [4] S. Fukuda and T. Yoda, "A novel current-tracking method for active filters based on a sinusoidal internal model," *IEEE Trans. Ind. Appl.*, vol. 37, pp. 888–895, 2001.
- [5] H. Komurcugil and O. Kukrer, "A new control strategy for single-phase shunt active power filters using a Lyapunov function," *IEEE Trans. Ind. Electron.*, vol. 53, no. 1, pp. 305–312, Dec. 2006.
- [6] L. Asiminoaei, F. Blaabjerg, and S. Hansen, "Detection is key—Harmonic detection methods for active power filter applications," *IEEE Ind. Appl. Mag.*, vol. 13, no. 4, pp. 22–33, Jul./Aug. 2007.
- [7] J.-C. Wu and H.-L. Jou, "Simplified control method for the single-phase active power filter," *Proc. IEE*, vol. 143, no. 3, pp. 219–224, May 1996.
- [8] D. Torrey and A. Al-Zamel, "Single-phase active power filters for multiple nonlinear loads," *IEEE Trans. Power Electron.*, vol. 10, no. 3, pp. 263–272, May 1995.
- [9] L. P. Kunjumammed and M. K. Mishra, "A control algorithm for single-phase active power filter under non-stiff voltage source," *IEEE Trans. Power Electron.*, vol. 21, no. 3, pp. 822–825, May 2006.
- [10] C. Zhang, C. Qiaofu, Z. Youbin, L. Dayi, and X. Yali, "A novel active power filter for high-voltage power distribution systems application," *IEEE Trans. Power Del.*, vol. 22, no. 2, pp. 911–918, Apr. 2007.
- [11] M. Cirrincione, M. Pucci, and G. Vitale, "A single-phase dg generation unit with shunt active power filter capability by adaptive neural filtering," *IEEE Trans. Ind. Electron.*, vol. 55, no. 5, pp. 2093–2110, May 2008.
- [12] A. Nasiri, S. B. Bekiarov, and A. Emadi, "A new reduced parts on-line single-phase ups system," in *Proc. IEEE 29<sup>th</sup> Annu. Conf. Ind. Electron. Soc.*, vol. 1, 2003, pp. 688–693.
- [13] A. Nasiri, S. B. Bekiarov, and A. Emadi, "Reduced parts single-phase series-parallel ups systems with active filter capabilities," *25th Int. Telecommun. Energy Conf.*, pp. 366–372, 2003.
- [14] A. Nasiri, S. B. Bekiarov, and A. Emadi, "Reduced parts three-phase series-parallel ups system with active filter capabilities," in *Proc. 38th IAS Annu. Meeting Conf. Rec. Ind. Appl. Conf.*, vol. 2, Oct. 2003, pp. 963–969.
- [15] A. Nasiri, "Digital control of three-phase series-parallel uninterruptible power supply systems," *IEEE Trans. Power*

Electron., vol. 22, no. 4, pp. 1116–1127, Jul. 2007.

[16] W. Nogueira Santos, E. Cabral da Silva, C. Brandao Jacobina, E. de Moura Fernandes, A. Cunha Oliveira, R. Rocha Matias, D. Franca Guedes Filho, O. Almeida, and P. Marinho Santos, “The transformerless single-phase universal active power filter for harmonic and reactive power compensation,” *IEEE Trans. Power Electron.*, vol. 29, no. 7, pp. 3563–3572, Jul. 2014.

[17] L. Limongi, L. da Silva Filho, L. Genu, F. Bradaschia, and M. Cavalcanti, “Transformerless hybrid power filter based on a six-switch two-leg inverter for improved harmonic compensation performance,” *IEEE Trans. Ind. Electron.*, vol. 62, no. 1, pp. 40–51, Jan. 2015.

[18] W. Nie and Z. Wang, “A research on circuit topology of new single-phase dual inverters ups,” in *Proc. Int. Conf. Comput. Sci. Service Syst.*, Jun. 2011, pp. 1971–1974.

[19] E. R. da Silva, W. R. dos Santos, C. B. Jacobina, and A. C. Oliveira, “Single-phase uninterruptible power system topology concepts: Application to an universal active filter,” in *Proc. IEEE Energy Convers. Cong. Expo.*, Sep. 2011, pp. 3179–3185.

[20] S. da Silva, R. Barriviera, R. Modesto, M. Kaster, and A. Goedel, “Single-phase power quality conditioners with series-parallel filtering capabilities,” in *Proc. IEEE Int. Symp. Ind. Electron.*, Jun. 2011, pp. 1124–1130.